remote sensing

MDPI

Project Report

Earth Observation to Investigate Occurrence, Characteristics and Changes of Glaciers, Glacial Lakes and Rock Glaciers in the Poiqu River Basin (Central Himalaya)

Tobias Bolch [1,*], Tandong Yao [2], Atanu Bhattacharya [1,3], Yan Hu [4], Owen King [1], Lin Liu [5], Jan B. Pronk [1], Philipp Rastner [6] and Guoqing Zhang [2]

1 School of Geography and Sustainable Development, University of St Andrews, St Andrews KY16 9AL, Scotland, UK; atanu.bhattacharya@jisuniversity.ac.in (A.B.); ogak1@st-andrews.ac.uk (O.K.); janboukepronk@gmail.com (J.B.P.)
2 State Key Laboratory of Tibetan Plateau Earth System Science, Resources and Environment, Institute of Tibetan Plateau Research, Chinese Academy of Sciences, Beijing 100101, China; tdyao@itpcas.ac.cn (T.Y.); guoqing.zhang@itpcas.ac.cn (G.Z.)
3 Department of Earth Sciences & Remote Sensing, JIS University, Kolkata 700109, India
4 Institute of Environment, Energy and Sustainability, The Chinese University of Hong Kong, Hong Kong 999077, China; huyan@link.cuhk.edu.hk
5 Earth System Science Programme, Faculty of Science, The Chinese University of Hong Kong, Hong Kong 999077, China; liulin@cuhk.edu.hk
6 Department of Geography, University of Zurich, 8057 Zurich, Switzerland; philipp.rastner@geo.uzh.ch
* Correspondence: tobias.bolch@st-andrews.ac.uk

check for updates

Citation: Bolch, T.; Yao, T.; Bhattacharya, A.; Hu, Y.; King, O.; Liu, L.; Pronk, J.B.; Rastner, P.; Zhang, G. Earth Observation to Investigate Occurrence, Characteristics and Changes of Glaciers, Glacial Lakes and Rock Glaciers in the Poiqu River Basin (Central Himalaya). *Remote Sens.* **2022**, *14*, 1927. https://doi.org/10.3390/rs14081927

Academic Editors: José Darrozes and Stefano Urbini

Received: 31 January 2022
Accepted: 13 April 2022
Published: 15 April 2022

Publisher's Note: MDPI stays neutral with regard to jurisdictional claims in published maps and institutional affiliations.

Abstract: Meltwater from the cryosphere contributes a significant fraction of the freshwater resources in the countries receiving water from the Third Pole. Within the ESA-MOST Dragon 4 project, we addressed in particular changes of glaciers and proglacial lakes and their interaction. In addition, we investigated rock glaciers in permafrost environments. Here, we focus on the detailed investigations which have been performed in the Poiqu River Basin, central Himalaya. We used in particular multi-temporal stereo satellite imagery, including high-resolution 1960/70s Corona and Hexagon spy images and contemporary Pleiades data. Sentinel-2 data was applied to assess the glacier flow. The results reveal that glacier mass loss continuously increased with a mass budget of -0.42 ± 0.11 m w.e.a^{-1} for the period 2004–2018. The mass loss has been primarily driven by an increase in summer temperature and is further accelerated by proglacial lakes, which have become abundant. The glacial lake area more than doubled between 1964 and 2017. The termini of glaciers that flow into lakes moved on average twice as fast as glaciers terminating on land, indicating that dynamical thinning plays an important role. Rock glaciers are abundant, covering approximately 21 km^2, which was more than 10% of the glacier area (approximately 190 km^2) in 2015. With ongoing glacier wastage, rock glaciers can become an increasingly important water resource.

Keywords: Himalaya; glacier changes; glacier velocity; geodetic method; glacial lakes; rock glacier

1. Introduction

Meltwater from the cryosphere contributes a significant fraction of the freshwater resources in China and in the countries receiving water from the mountains of Asia, also called the Third Pole [1]. However, glaciers in most parts of High Mountain Asia (HMA) are shrinking and loosing mass, and permafrost is thawing as in most other areas on Earth, endangering reliable water supply [2–5]. Retreating glaciers allow proglacial lakes to develop behind their terminal moraines or in overdeepenings carved by the erosional power of the ice. These proglacial lakes can further increase glacier mass loss [6,7] but also pose a serious threat to downstream communities and infrastructure [8,9]. Debris-covered glaciers which are prone to lake development [10] are abundant in the Himalaya [11,12]. Even

though a thick layer of debris insulates the ice, debris-covered glaciers in the Himalaya have been found to lose mass at similar or even higher rates than debris-free glaciers [6,13,14]. Rock glaciers are another important component of the cryosphere and are abundant in the Himalaya and elsewhere in most parts of HMA [15–17]. They are characteristic landforms located in the permafrost environment, contain a significant amount of ice, and show cumulative deformation [17,18].

Remote sensing is an effective tool to identify and investigate the characteristics and changes the different components of the cryosphere as well as glacial lakes. This is particularly true as they are located in remote mountain areas that are often difficult or impossible to access on the ground [19–21]. Multitemporal optical satellite data such as ASTER, Landsat or Sentinel-2 have been widely used to map glaciers and glacial lakes and their changes on local [22–25], large regional [26–28] and even global scale [29,30] since the 1980s. These multi-temporal data also allow glacier surface velocities to be investigated [31–33]. While Landsat has the advantage of temporal coverage since the 1980s, the higher spatial resolution of Sentinel-2 (10 m vs. 30 m) available since 2015 allows higher accuracy and smaller glaciers and glacial lakes to be examined [34,35]. The analysis of multi-temporal digital elevation models (DEMs) is the most effective way of investigating glacier mass budget changes over broad spatial and temporal scales. This commonly used approach is a geodetic method that has been widely applied at local [36,37], regional [38–40] and even global level [41] to study glacier mass changes. Regional and global estimates have been available since the year 2000, when spatially and temporally resolved observations of glacier height changes became possible thanks to constantly orbiting stereoscopic satellite sensors such as ASTER and the SRTM DEM, commencing 11–18 February 2000 during a dedicated Space Shuttle Mission [42]. The assessment of geodetic glacier mass balance previous to 2000 is more difficult due to a scarcity of appropriate data, data quality issues within available datasets and data access limitations. Recent advances in image processing techniques have begun to unlock the potential held in the earliest stereoscopic satellite image archives, such as Corona KH-4 (operational 1962–1972) and KH-9 (1971–1986), which have been proven to enable longer-time series ([6,43–46]). In combination with data from more modern sensors (e.g Pléaides, Satellite pour l'Observation de la Terre-SPOT, ASTER), these data have the potential to yield a record of glacier mass fluctuations across six decades, in turn-providing information regarding the long-term response of the high-mountain environment to climate change [36,47,48].

The main aim of the work conducted within the framework of the Dragon 4 project was to study the cryosphere and its changes in different regions in HMA and understand different drivers of the changes. We therefor mapped glaciers and rock glaciers, estimated glacier velocities and investigated long-term glacier mass changes and changes in glacial lakes, along with analysis of climatic data. In this paper, we focus on the Poiqu River Basin (hereafter called the Poiqu basin), located in central Himalaya where comprehensive investigations, including joint field work, were conducted by European and Chinese scientists, and where multi-temporal high resolution satellite data was available.

The Poiqu basin covers approximately 2000 km^2 and drains from the Tibetan Plateau in the north into Nepal in the south (lowest elevation at the border is 1540 m above sea level, a.s.l.). The northern water divide is approximately 5500 m a.s.l., and many mountain peaks exceed 7000 m a.s.l., with the highest peak being Mt. Shishapangma (8024 m a.s.l.) (Figure 1). Consequently, the overall mean elevation is relatively high (~4970 m a.s.l.). The climate is largely influenced by the Indian monsoon. ERA5 Land data analysis revealed a mean annual air temperature (MAAT) of −2.4 °C at the mean elevation of the basin and a mean annal precipitation average over the whole basin of approximately 1710 mm, with more than 80% of the precipitation occurring in the summer [47]. The glaciers are located at a much higher elevation than the weather station; it can therefore be assumed that the glacier are of summer-accumulation type. Long term measurements at Nyalam (also called Nielamu) weather station have an average of 3.8 °C at 3750 m a.s.l. [49]. The 0°-isotherm is located at approximately 4300 m a.s.l. and the equilibrium line altitude (ELA) of the glaciers

at about 5600 m a.s.l. [2,43,50]. The temperature measured at Nyalam station increased on average by 0.24 °C per decade, along with a slight precipitation decrease (−7.6 mm per decade) [49].

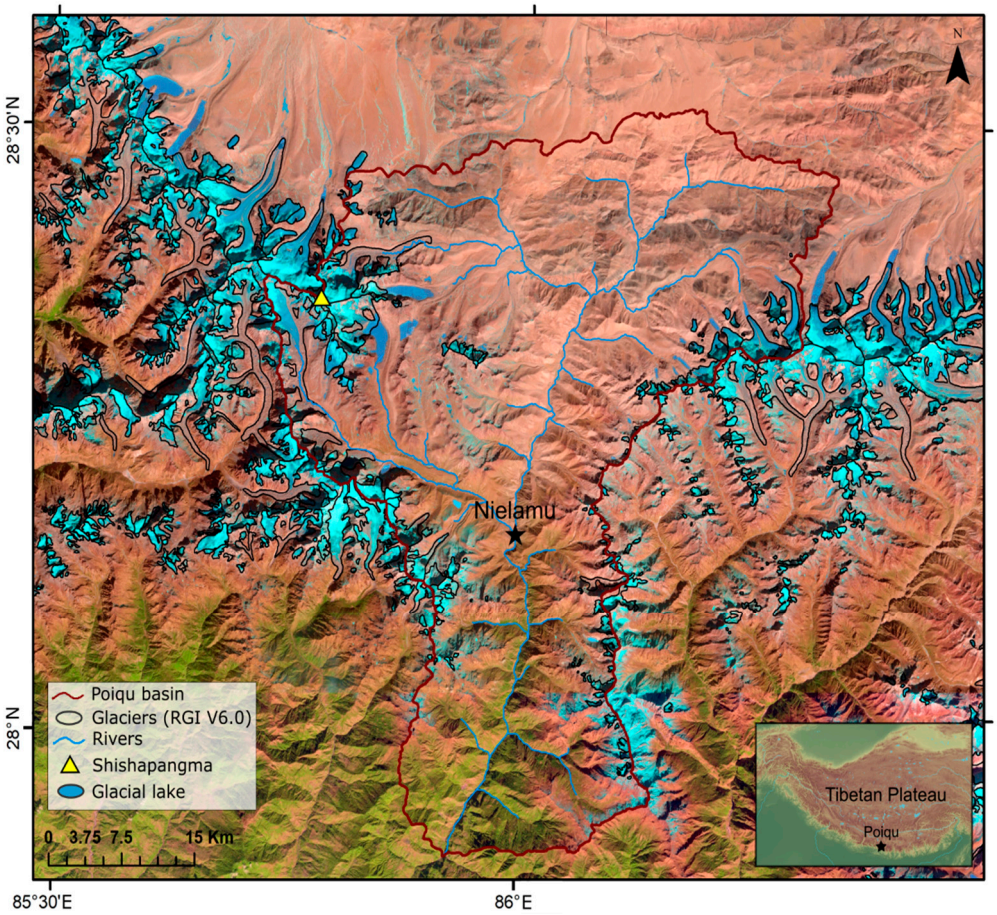

Figure 1. Study region, its glaciers and glacial lakes; background image: Sentinel-2 MSI image mosaic from Dec 2021, false colour composite (SWIR-NIR-RED).

2. Project, Sub-Projects, EO and Other Data Utilisation

2.1. List of Sub-Projects and Teaming

The overall project to study the cryosphere and its changes in different regions in HMA was subdivided into the four subprojects according to the investigated features and topics a: (1) glacial lakes, (2) glacier mass changes, (3) glacier velocity and (4) rock glaciers. The team consisted of researchers from the University of St Andrews, UK, and the University of Zurich, Switzerland, as well as the Institute of Tibetan Plateau Research, Beijing, China and the Chinese University of Hongkong, China.

2.2. Description and Summary Table of Earth Observation and Other Data Utilized

The data used are based on medium-high to very-high resolution remotely-sensed optical and radar imageries acquired between 1964 and 2018 (Table 1). Glacial lake mapping and glacier surface elevation changes were estimated by using imageries collected by Corona KH-4A (spatial resolution 2.7 m), Hexagon-KH9 (7.6 m), Advanced Spaceborne Thermal Emission Reflection Radiometer (ASTER) (15 m), Pléiades (0.5 m) and SPOT-7 (1.5 m) [6,47,49,51]. Additionally, to identify the rock glacier activity, ALOS-1 PALSAR fine-beam mode L-band (10 m) radar imageries were utilised [51]. Glacier surface velocity was estimated by Sentinel-2 MSI (10 m) imageries [52]. Moreover, several Landsat archives were explored, including Thematic Mapper (TM) (30 m), Enhanced Thematic Mapper plus (ETM+) (30 m multispectral, 15 m in the panchromatic band) and Operational Land

Imager (OLI) (30 m multispectral, 15 m panchromatic band) for glacier and glacial lake mapping [45]. The details of remote sensing imagers are their usages are presented in Table 1.

Table 1. Satellite data used within this study.

Satellite	Sensor	No. of Scenes	Date	Scene IDs	Usage
Corona KH-4A		7	26/11/1964	DS1014-2118DA188 DS1014-2118DA189 DS1014-2118DA190 DS1014-2118DA191 DS1014-2118DF187 DS1014-2118DF188 DS1014-2118DF189	Glacial lakes, DEM [1], GMB [2]
Hexagon	KH9 MC	2	23/11/1974	DZB1209-500101L006001 DZB1209-500101L007001	Glacial lakes, DEM [1], GMB [2]
Terra	ASTER	8	23/09/2004 16/10/2004 23/10/2009 20/10/2017 26/10/2019	AST_L1A_00309232004045839_20191216041641_19157 AST_L1A_00309232004045848_20191216041641_19161 AST_L1A_00310162004050426_20191216041651_19216 AST_L1A_00310162004050435_20191216041651_19218 AST_L1A#00310232009045933_10262009104316 AST_L1A#00310232009045924_10262009104307 AST_L1A#00310202017050548_10212017083708 AST_L1A#00310262019050517_10272019083336	DEM [1], GMB [2]
ALOS	PALSAR	7	16/07/2007 31/08/2007 16/10/2007 16/01/2008 02/03/2008 02/06/2008 18/07/2008	ALPSRP078570550 ALPSRP085280550 ALPSRP091990550 ALPSRP105410550 ALPSRP112120550 ALPSRP125540550 ALPSRP132250550	Rock glacier activity
Landsat	TM/ETM+/OLI	107	1988–2017	For details see [49]	Glaciers, glacier velocity, glacial lakes
Pléiades	1A/1B	10	25/09/2018 26/09/2018 27/09/2018 03/10/2018 15/10/2018 15/10/2018 02/10/2018 03/11/2018 04/11/2018 02/10/2018	DS_PHR1A_201809250511185_FR1_PX_E085N28_1110_03316 DS_PHR1B_201809260504010_FR1_PX_E086N28_0105_05430 DS_PHR1A_201809270456239_FR1_PX_E086N28_0510_01804 DS_PHR1B_201810030500231_FR1_PX_E086N28_0309_02182 DS_PHR1B_201810150507481_FR1_PX_E085N28_1103_02921 DS_PHR1B_201810150507593_FR1_PX_E086N27_0123_00862 DS_PHR1B_201810220504174_FR1_PX_E086N28_0102_01804 DS_PHR1B_201811030511344_FR1_PX_E085N28_0715_03053 DS_PHR1A_201811040503518_FR1_PX_E085N28_1108_01768 DS_PHR1A_201810020508169_FR1_PX_E085N28_0911_05204	DEM [1], GMB [2] rock glacier mapping
SPOT-7	HRVIR	1	06/10/2015	DS_SPOT7_201510060438227_FR1_FR1_SE1_SE1_E086N28_01303	DEM [1], GMB [2]
Sentinel 2	MSI	149	Nov 2016–Nov 2019	For details see [52]	Glacier velocity

[1] Generation of digital elevation model, [2] Calculation of glacier mass balance.

3. Background, Research and Approach for the Different Topics

3.1. Glacial Lakes

3.1.1. Background and Research Aims

Glacial lakes emerge with glacier retreat, either by filling overdeepenings carved by the erosional power of glaciers or the proglacial area behind the terminal moraine (Figure 2). These glacial lakes impact glacier mass loss [6,7], and glacial lake outburst floods (GLOFs) can occur in the case of a breach of the damming moraines. They can have severe impacts to the downstream area and infrastructure [8,14,53] At least eight major GLOFs with strong impacts have been recorded in the Poiqu basin, including repeating GLOF events from Jialong Co and Cirenam Co, e.g., [54,55]. This basin has been identified as an area with one of the highest dangers of GLOFs in HMA [8,56]. Knowledge regarding the occurrence and changes of glacial lakes is important for understanding the evolution of glaciers and glacial lakes and to estimate the likelihood of GLOF occurrence. The main aims of the investigations were therefore to map glacial lakes and to generate a detailed time series of their changes using multi-temporal satellite data acquired since the 1960s.

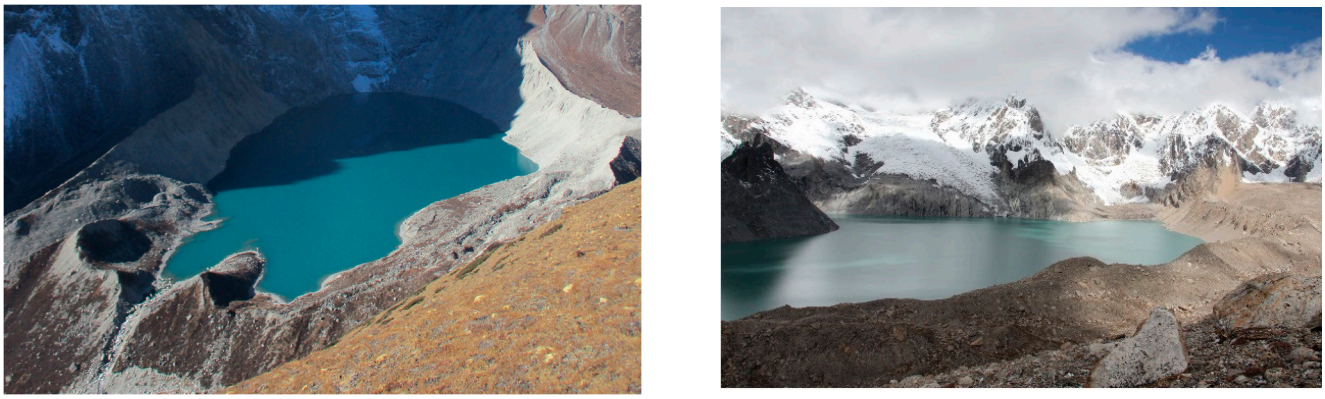

Figure 2. Jialong Co (**left**, photo: T. Bolch) and Garlong Co (**right**: photo: J.B. Pronk), moraine-dammed proglacial lakes located in the Poiqu River Basin.

3.1.2. Research Approach

Glacial lakes were mapped using 1964 Corona KH-4A declassified spy imagery (spatial resolution ca 2.7 m), 1974 Hexagon KH-9 (ca. 7 m) and a detailed time series from 1988 to 2017 of Landsat TM/ETM+/OLI images (30/15 m) (Table 1). The only available cloud-free declassified data were acquired in November, but the lakes were well identifiable nevertheless. The lakes were delineated manually based on panchromatic KH-4A and KH-9 images. The lakes were automatically identified using the Landsat scenes from each year with the best snow and cloud conditions (usually acquired at the end of the ablation and Monsoon period, end August/beginning of September) based on the Normalised Difference Water Index (NDWI, green-NIR/green + NIR) [57]. An alternative NDWI using the blue band instead of the green band was suggested to map glacial lakes [23]. The different NDWIs were widely used for glacial lake mapping (e.g., [29,43,58]). The minimum size threshold was set at 0.007 km^2. The mapping results were visually checked based on the same and additional available scenes, and misclassifications were manually rectified. We visually classified the lakes into moraine-dammed, bedrock dammed and supra-glacial lakes. For more information, refer to Zhang et al. (2019) [49].

3.2. Glaciers: Mass Changes

3.2.1. Background and Research Aims

Glaciers react sensitively to climatic variations and are therefore good climatic indicators in elevations where weather stations are rare or not existing. Moreover, they contribute to river runoff and are an important and reliable source of water, particularly for the arid regions surrounding the mountains [1,5,59] or in dry periods or periods of droughts [60].

In most parts of the Himalayas, the main accumulation season for glaciers is during the summer monsoon, coinciding with the main ablation season. As a result, peak runoff from glaciers is similar in timing to peak runoff from pluvial segments [61]. However, even though the timing is similar, glacier melt provides reliable runoff while monsoon precipitation can have high interannual variations [5,60]

With increasing glacier mass loss, the glacier runoff initially increases, but with further shrinking glaciers the runoff decreases after a tipping point is reached. This time of "peak water" is projected for the next decades for most large Asian river catchments but is already over in less glacierised catchments with smaller low-lying glaciers [4,62]. The utilised glacio-hydrological models are calibrated and validated using past observations and detailed, and long-term observations are required to improve the projections.

In this subproject, we therefore aimed to generate the longest possible time series of geodetic glacier mass balance estimates from available archives of optical stereo imagery. Using these data, we aimed to examine the response of glaciers in the Poiqu basin, along with those in the Himalaya as a whole, to both changes in climate (temperature, precipitation) and glacier morphology (proglacial lake development). Collectively, we aimed to disentangle the impact of climatic and non-climatic factors on glacier mass budgets in the Poiqu basin and beyond in order to better understand the likely future evolution of glaciers in the region under continued climate change.

3.2.2. Research Approach

We derived a time series of DEMs covering the Poiqu basin using imagery from the Hexagon KH-9, ASTER and Pléiades sensors (Table 1) [47]. These multi-temporal DEMs provided a record of glacier surface elevation change spanning two periods over 44 years (1974–2004, 2004–2018). The earlier study [6] used similar Hexagon data but used SRTM and HMA DEM instead of ASTER and Pléiades data. From the DEM difference grid, we generated geodetic mass balance estimates following established processing steps (e.g., co-registration, outlier filtering, gap filling) and volume-to-mass conversion [45,63–66]. DEM coverage allowed for the derivation of glacier mass loss estimates for 148 glaciers in the basin (71% total glacier area) over the two time periods. In order to obtain more detailed information about the evolution of mass changes, we compiled a time series for the adjacent Langtang valley where data from a previous study [67] and suitable Corona scenes were available. The available DEMs allowed us to cover a time span of more than 50 years (1964–2018), with six subperiods. For more information, refer to King et al. (2019) [6] and Bhattacharya et al. (2021) [47].

In order to assess the impact of climate change on glaciers, we compiled a time series of meteorological observations (Nielamu, 3810 m a.s.l) and reanalysis data (ERA5 Land). We examined the correlation between summer temperature and solid precipitation anomalies and glacier mass budgets to decipher the impact of climatic change on glacier mass budget perturbations (cf. [47]). Similarly, we examined the differences in glacier mass loss rates from glaciers of two different terminus types: those terminating into a large proglacial lake and those terminating on land (cf. [6,52]).

3.3. Glacier Velocity

3.3.1. Background and Research Aims

Long-term glacier mass changes induce substantial variability in glacier flow, which in turn impacts ice fluxes and glacier hypsometry (the distribution of ice with elevation). As with glacier surface elevation change, remote sensing is by far the most powerful tool with which we can assess large scale fluctuations in glacier flow in response to climate change. The tracking of features present at glacier surfaces between pairs of images separated by a few weeks, months or even years is a commonly applied method of deriving glacier surface velocity fields [68,69]. Dehecq et al. (2019) [70] derived HMA-wide glacier surface velocity estimates by employing feature tracking on Landsat image pairs. Whilst the Landsat archives provide unparalleled spatial and temporal coverage of earth-surface conditions

over the last few decades, the recent operation of the Sentinel-2 satellites has improved the spatial, radiometric and temporal resolution at which we can observe the cryosphere. Improvements in our capability to resolve glacier flow are particularly important in high mountain regions, where the extreme topography and snow cover limits the accuracy and coverage of glacier velocity fields.

The main aim of this subproject was to derive Himalaya-wide glacier surface velocity estimates for a contemporary time period using Sentinel-2 imagery. Using these data, we aimed to examine the variability of glacier flow depending on glacier morphology, aspect, surface cover and terminus type. Within this paper, the main aim is to present the results for the Poiqu basin and put them into the context of the wider Himalaya.

3.3.2. Research Approach

We used, in particular, the 10-m near-infrared band (band 8) from the Sentinel-2 imagery, which is well suited for tracking the features on glaciers due to the contrasting spectral properties of fresh snow and firm and clean ice at this wavelength [35]. The higher resolution compared to Landsat sensors allowed us to work with glaciers larger than 3 km^2, compared to the 5 km^2 previously utilized by [70]. This enabled us to add substantially more glaciers to our dataset. We classified glaciers as lake-terminating when the glacier shows a clear terminal ice cliff in direct contact with the lake, and we based our classification on the glacial-lake inventory of [21,49]. We selected multiple image pairs of the same locality to maximize the velocity field coverage. The final velocity field is an average of all the valid velocity estimates, a strategy successfully explored by several studies (i.e., [31,71]). In this study, we used the orientations-correlated feature-tracking method, as this method has proven to perform best under most circumstances [33]. We matched the orientation of the intensity gradient that is contained in the phase of the orientation image by correlating the images in the frequency domain with fast Fourier transforms (FFTs). After this initial estimate, we then refined the maximum estimation by up-sampling the product of the two orientation images in the frequency domain in a small neighbourhood of the initial maximum [72]. To assess the uncertainty in the velocity field and to reduce systematic offsets in the x- and y-displacement fields, a large 100 km $\times$ 100 km stable area was selected, of which we could reasonably assume the displacement to be zero. For further information, refer to Pronk et al. (2021) [52]. The results of this study were compared to earlier results calculated based on Landsat OLI panchromatic images from 2013–2017 using COSI-Corr [68] for the Poiqu basin within the study of Zhang et al. (2019) [49].

3.4. Rock Glaciers: Occurrence, Characteristics and Mapping Challenges

3.4.1. Background and Research Aims

Rock glaciers are distinctive geomorphological landforms located in permafrost environments and produced by cumulative deformation through long-term viscous creep of perennially frozen angular rocks (talus, moraines) rich in ice [17,18,73]. Rock glaciers are commonly classified into three groups according to their kinematic status and amount of the internal ice: active, inactive and relict. In addition, they can be separated into talus-derived and moraine-derived rock glaciers [17]. Different opinions regarding the origin of the ice have been proposed, but it is commonly accepted that rock glaciers are related to permafrost occurrence [74]. Rock glaciers contain a significant amount of ice and can therefore provide a relevant contribution to water supply and alter river runoff [16,17,75]. Knowledge regarding rock glacier characteristics and occurrence has increased during the last few years globally and also in HMA [16,76–78], but there are still many missing regions, including the Poiqu basin. Moreover, mapping approaches and definitions also vary between the studies, which thus constitutes a major problem in rock glacier inventories [79]. The main aim of this research was to generate a consistent rock glacier inventory for the Poiqu basin using available very-high-resolution Pléiades images and related generated DEMs and characterise the activity and occurrence of the landforms based on the Pléiades and InSAR data.

3.4.2. Research Approach

Automated methods to identify rock glaciers, such as using deep learning and object-based image analysis techniques are in development (e.g., [72,80]), but are associated with high uncertainties and are not yet suited for accurate mapping. Manual delineation is therefore the most accurate method to identify rock glaciers. A high resolution is important to be able to correctly identify the geomorphological landforms and distinguish them from similar looking landforms, such as rock fall deposits [79].

We used very-high-resolution Pléiades data and a hillshade based on the generated Pléiades DEM (see Section 3.2) to manually digitise the outlines. Images available from Google Earth were used as additional information. The DEM was also used to extract topographic information about the rock glaciers. The activity status was determined with the help of InSAR and was based on morphological indication. Radar interferograms were generated from the ALOS-1 PALSAR data by standard interferometric processing to find the line-of-sight (LOS) displacement of the ground surface. SRTM DEM was used to estimate and remove the topographic phases. Finally, an adaptive Goldstein filter (8×8 pixels) was used to mitigate the phase noise. Rock glaciers were classified as active in cases where fringes were observed in rock glaciers or parts of rock glaciers previously identified. Rock glaciers were further classified as active when the rock glacier front was steep and fresh looking or a clear ridges-and-furrow structure was visible. The rock glaciers were further classified as talus-derived or moraine-derived based on the visually identified source of rock material. For further information, refer to Rastner et al. (in review) [51].

4. Research Results

4.1. Glacial Lakes

The number of glacial lakes increased from 73 in 1984 to 99 in 2000. Thereafter the number remained, on average, similar (102 in 2017). Three lakes have a relatively large area, for example, Galong Co is the largest lake, with an area of ~5.5 km^2 in 2017, and the other two large lakes are Gangxi Co (4.5 km^2) and Gung Co (2.1 km^2). Four lakes (Jialong Co, Paquci, Youmojan Co, Cawuquden Co) have areas of each ~0.5 km^2. Sixteen lakes each have areas in the range of $0.1-0.5$ km^2, and another 79 lakes have small areas of less than 0.1 km^2.

The lake area doubled from 9.7 ± 0.1 km^2 in 1964 to 20.5 ± 0.4 km^2 in 2017. The area increase reduced after 2010 but was still evident. The area increase is particularly evident for the larger lakes (area ≥ 0.02 km^2; 64 lakes having been larger than this threshold in 2017) and moraine-dammed glacial lakes. The drop of the area increase rates after 2010 are mainly due to the fact that few lakes reached their maximum possible extent governed by the topography. Their parent glaciers retreated further, and their tongues are now located at the slopes above the lakes. It is also important to consider that several glacial lakes have experienced an outflow or even a GLOF, causing a significant area loss of these lakes (Figure 3). From historical records, we know that four lakes (Taraco, Cirenma Co, Jialong Co, and Gongbatongsha Tsho) have drained as a result of a GLOF [54,55].

4.2. Glacier Mass Changes

Glaciers in the Poiqu basin have thinned and retreated substantially over the last five decades, and their mass budget has been negative over the full study period as a result [6,47,49]. The mean glacier mass balance, derived by two individual studies contributing to the Dragon 4 project, match well (-0.36 ± 0.07 m w.e.a^{-1} for 1974–2018 cf. [47] and -0.33 ± 0.12 m w.e.a^{-1} for 1974–2017, cf. [49]), giving confidence in the results. Comparison of multi-temporal mass balance estimates shows that the rate of ice loss has increased substantially over the last 44 years. Between 1974 and 2004, the mean mass balance of glaciers in the basin was -0.30 ± 0.10 m w.e.a^{-1}. The rate of ice mass loss was approximately 40% higher between 2004 and 2018, when glaciers lost mass at a mean rate of -0.42 ± 0.10 m w.e.a^{-1} [47]. The Langtang valley (mean elevation ~5182 m) adjacent to the Poiqu basin experienced a slightly higher mass loss rate in the recent period

(-0.50 ± 0.11 m w.e.a^{-1} for 2004–2019) and a slightly lower one in the earlier time period (-0.24 ± 0.10 m w.e.a^{-1} for 1974–2004). The mass loss for the six individual periods constantly increased from -0.20 ± 0.09 m w.e.a^{-1} for 1964–1974 to -0.59 ± 0.114 m w.e.a^{-1} for 2017–2019 [47]. The debris-covered Langtang (G085816E28470N), maximum, minimum and mean elevations are 6617 m, 4506 m and 5333 m, respectively, and Langshisha (G085747E28200N) glaciers, maximum, minimum and mean elevations are 6375 m, 4530 m and 5270 m, respectively, and showed increased mass loss rates throughout the time span (-0.27 ± 0.10 m w.e.a^{-1} and -0.37 ± 0.10 m w.e.a^{-1} for 1964–2004, -0.62 ± 0.12 m w.e.a^{-1} and -0.61 ± 0.12 m w.e.a^{-1} for 2004–2019, respectively).

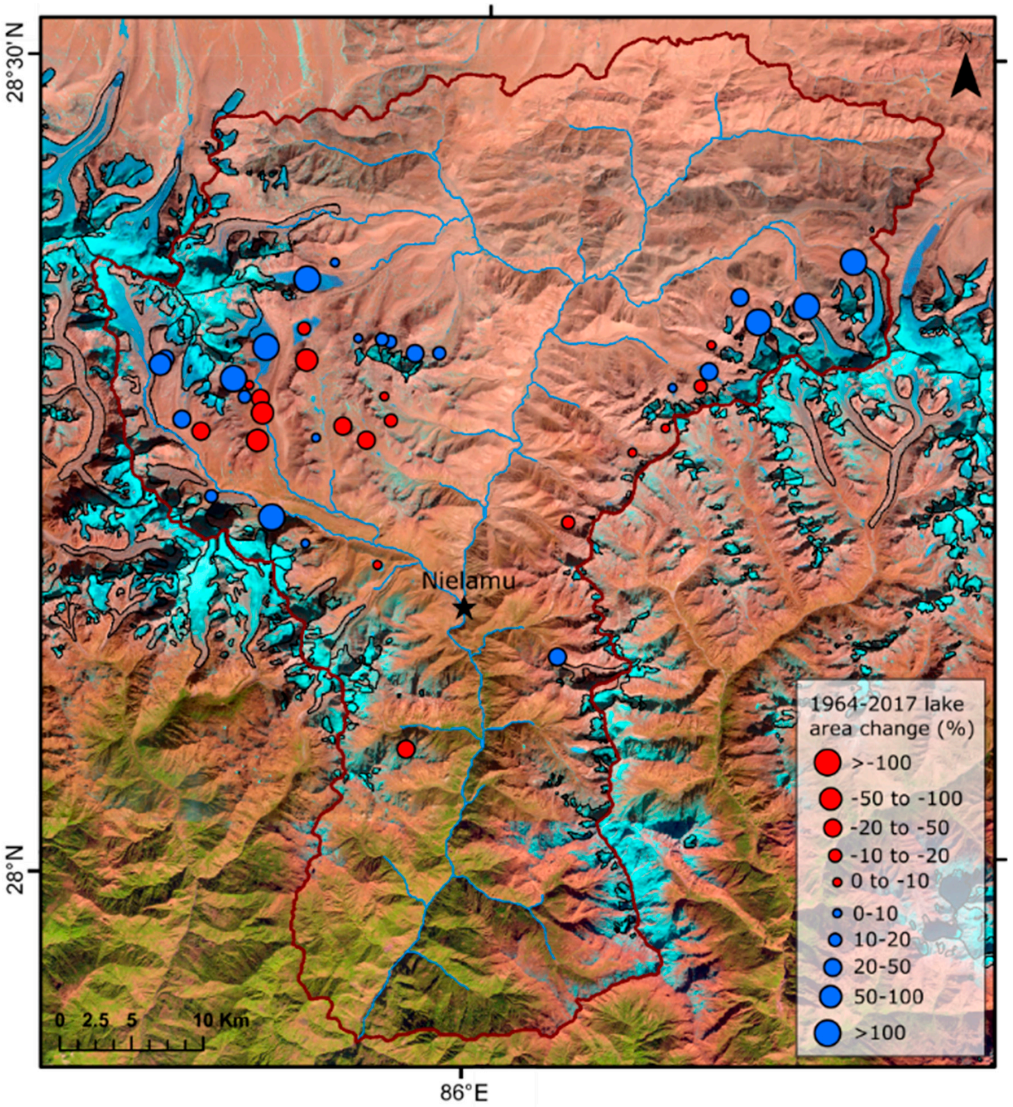

Figure 3. Area change of glacial lakes between 1964 and 2017 (data source: [42]).

A clear contrast was evident in the retreat and mass balance of glaciers of different terminus types in the Poiqu basin [6,49]. Both studies agree that glaciers terminating into proglacial lakes exhibited substantially higher rates of ice mass loss than glaciers terminating on land across both study periods. The higher surface elevation changes of most glaciers terminating in a lake can also be identified visually based on the DEM difference grid (Figure 4). Between 1974 and 2000, lake-terminating glaciers in the Poiqu basin lost ice at a mean rate of -0.36 ± 0.10 m w.e.a^{-1}, in comparison to land-terminating glaciers, which lost ice mass at a mean rate of -0.24 ± 0.10 m w.e.a^{-1} over the same time period. Between 2000 and ~2015, lake-terminating glaciers lost ice mass at a mean rate of -0.48 ± 0.12 m w.e.a^{-1}, compared to a rate of -0.35 ± 0.11 m w.e.a^{-1} for land-terminating

glaciers over the same time period [6]. Zhang et al. (2019) [49] report a more negative mass balance of -0.60 ± 0.04 m w.e.a^{-1} (elevation change -0.71 ± 0.05 m w.e.a^{-1}) for the eight glaciers which have been or are still in contact with glacial lakes.

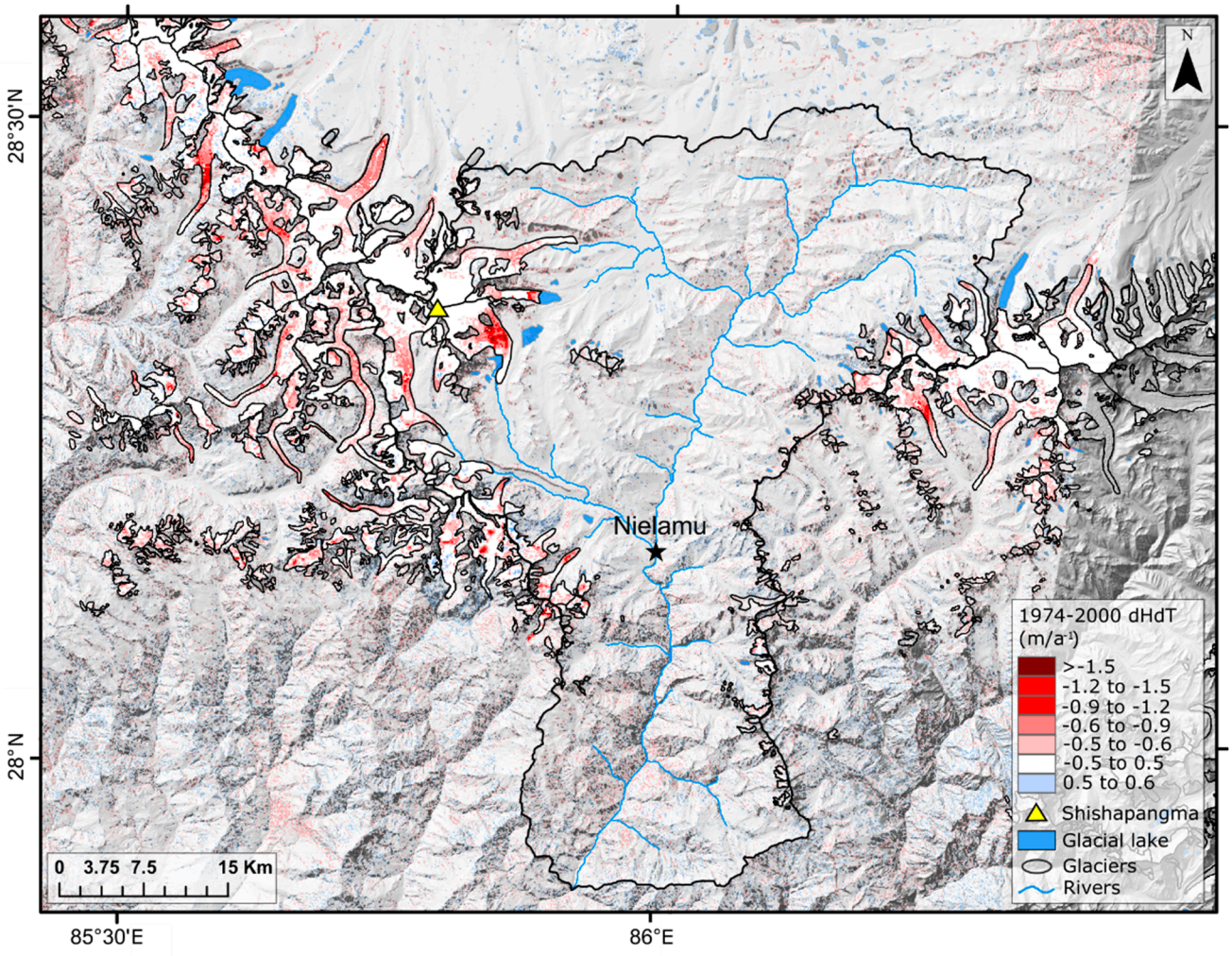

Figure 4. Glacier elevation changes in the Poiqu basin and surroundings (example): DEM difference between 1974 (KH9) and-2000 (SRTM Data) (data source: [6]).

Further analyses of the statistical characteristics of the sample of geodetic mass balance estimates generated revealed the evolving influence of proglacial lakes on glacier mass balance. Using unpaired, two-tailed t-tests, substantial differences in mass loss estimates for lake- and land-terminating glaciers were found within the Poiqu basin (mean -0.11 ± 0.04 m w.e.a^{-1}, 95% confidence interval, -0.20 to -0.02 m w.e.a^{-1}). This margin widened in the Poiqu basin between 2000 and 2015 (mean -0.14 ± 0.05 m w.e.a^{-1}, 95% confidence interval -0.25 to -0.04 m w.e.a^{-1}).

4.3. Glacier Velocity

The median velocity of the glaciers measured along the centreline below the ELA in the study region was 6.72 m yr^{-1} (IQR uncertainty range 6.61 to 6.83 m yr^{-1}). The median velocity of lake-terminating glaciers was 18.27 m yr^{-1} (17.75–18.68 m yr^{-1}), which is much higher than the median of all glaciers and of the land-terminating glaciers (5.44 (5.35–5.56) m yr^{-1}) [cf. [52]]. A slightly lower overall average glacier velocity of approximately 5 m yr^{-1} for the period 2013–2017 was found by [49] using Landsat data. This study also found significantly higher velocities of lake-terminating glaciers, which indicates the robustness of the finding.

The faster flow of the lake-terminating glaciers is also visually evident (Figure 5). Land-terminating glaciers become stagnant at the terminus, with only little velocity variation between the glaciers. In contrast, the median velocity of lake-terminating glaciers decreases only slightly towards the end but shows variation in dynamical behaviour (Figure 5, inset). An even stronger variability was found for the larger region with a substantially larger sample size (cf. [52]). Analysis of the possible aspect dependence of flow show large heterogeneities for lake-terminating glaciers. However, the highest velocities show glaciers flowing to the north. Further analysis of the aspect, slope, and area dependence of the velocity clearly show that the strong velocity contrast between land- and lake-terminating glaciers remain irrespectively from the topographic characteristics.

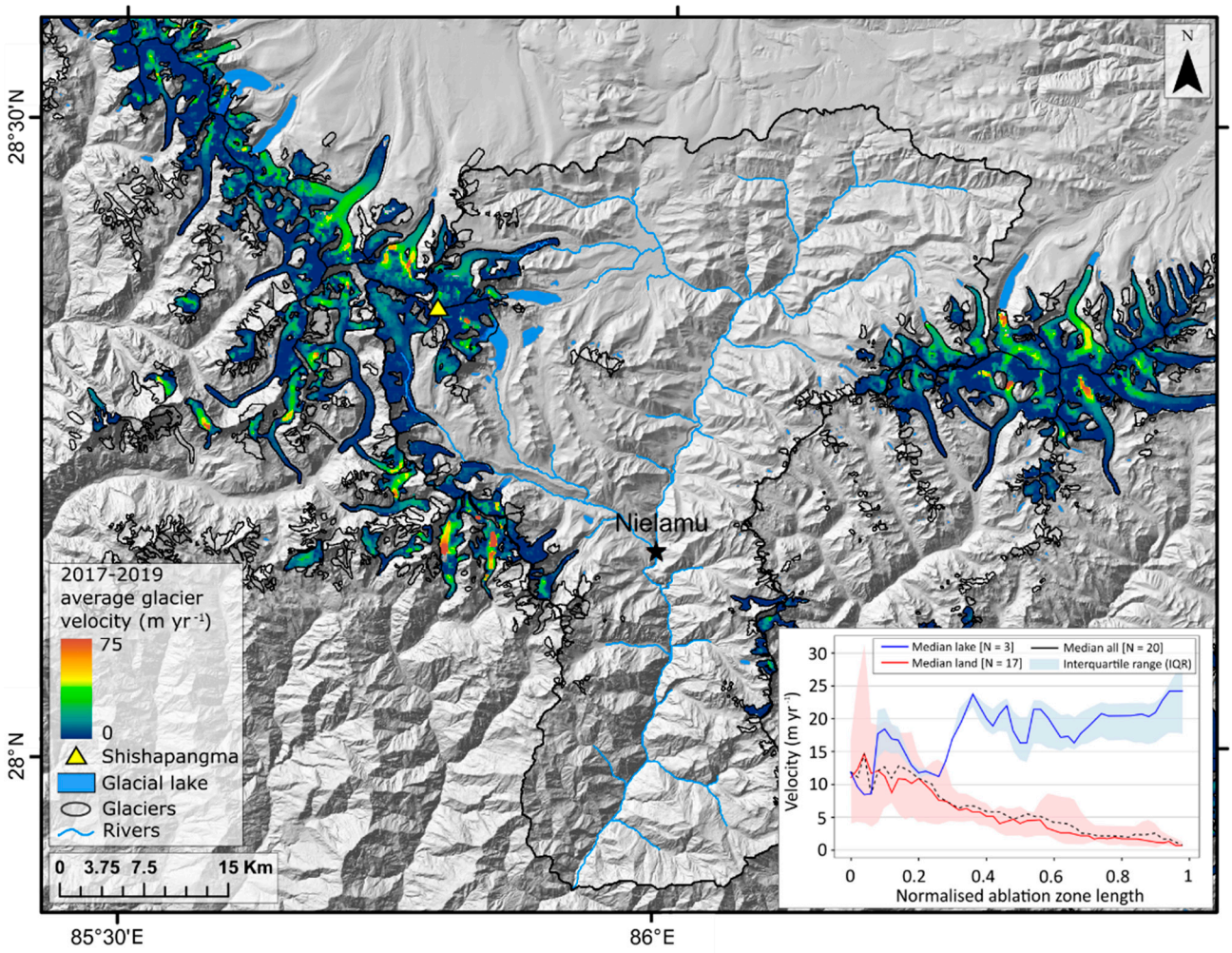

Figure 5. Surface velocity of glaciers in the Poiqu basin and surrounding area, inset: centreline velocities of the ablation areas of lake- and land-terminating glaciers in the Poiqu River basin (data source: [52]).

4.4. Rock Glaciers

We could identify 370 rock glaciers with an area of approximately 20.9 km^2 (mean area ~ 0.05 km^2), out of which 148 were identified as active (total area ~12.5 km^2, mean area: ~0.08 km^2) and 222 as inactive (~8.4 km^2, ~0.04 km^2) (Figure 6). The two largest rock glaciers cover ~0.5 and ~0.45 km^2. Most of the rock glaciers are talus-derived (n = 297, total area: ~15.5 km^2), much less are moraine-derived (n = 40, ~3.2 km^2) and 33 (~2.2 km^2) are not classifiable. Talus-derived rock glaciers are, on average, steeper (19.7°) but are smaller in size (~0.05 km^2) as compared to moraine-derived rock glaciers (17.8°, ~0.08 km^2). The rock glaciers are located between ~4000 m and ~6000 m a.s.l., with a mean elevation of

~5100 m a.s.l. For comparison, the mean glacier elevation is between 5300 and 5400 m a.s.l., with the lowest termini being at 4500 m a.s.l. Their location shows a correlation with elevation. This coincides with decreasing precipitation and increasing average elevation of the study region. The active rock glaciers are located slightly higher (average 5041 m a.s.l.) than the inactive ones (5008 m a.s.l.). The mean slope of all rock glaciers is 19.3°. The active ones are, on average, slightly steeper (19.7°) than the inactive rock glaciers (19.0°).

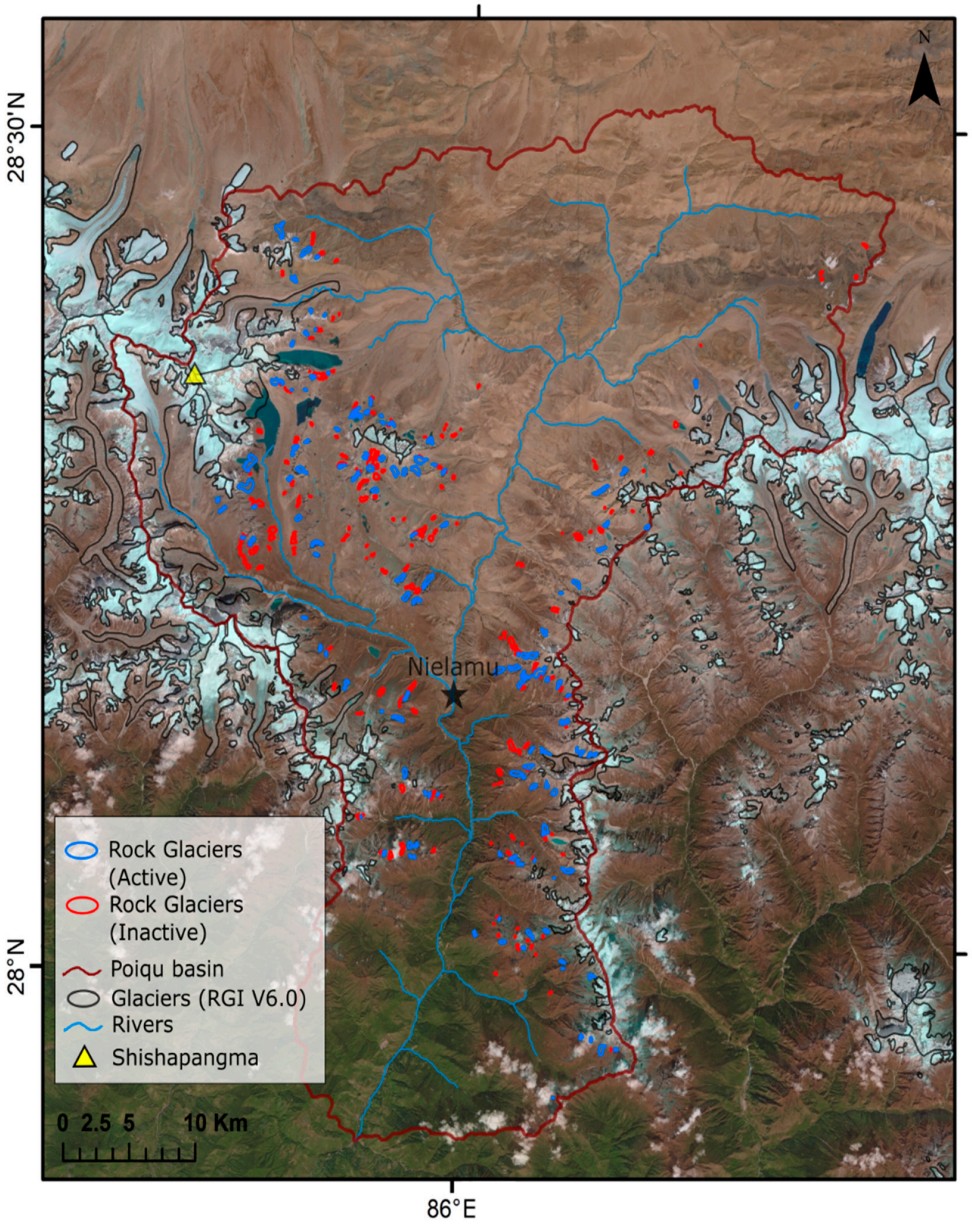

Figure 6. Rock glacier inventory of the Poiqu basin, background image: True colour composite of a Sentinel-2 image, acquired 12 September 2016 (data source: [51]).

5. Discussion and Conclusions

Our results revealed that the glaciers have significantly lost mass at an accelerating rate, and the number and area of glacial lakes have both increased concomitantly in the Poiqu basin since the 1960s. These findings are well in line with the reported changes of glacial lakes in the Himalaya (e.g., [81], the Tibetan Plateau [26], whole HMA [27] and the global trend [29]). However, the vast majority of the available studies are based on Landsat data and only a few periods. In contrast, the study performed within the Dragon 4 project provides information starting from the 1960s and offers the most comprehensive time series

with partially annual resolution since the late 1980s [49]. This allowed detailed insights in the lake evolution and showed that several glacial lakes reached their potential topographic maximum. This is important to consider for future modelling.

The results of geodetic mass balance studies in the Poiqu basin clearly show that substantial ice mass has been lost over the last five decades and that the rate of ice loss has increased throughout the study period. The mean mass balance of glaciers since the millennium in the Poiqu region (-0.42 ± 0.10 m w.e.a^{-1}) is substantially more negative than that of all glaciers across HMA (-0.18 ± 0.04 m w.e.a^{-1}, [82]) and is comparable to the mean global glacier mass balance over the same time period (-0.47 ± 0.20 m w.e.a^{-1} [83]). Increasing mass loss are also reported elsewhere in the Himalaya based on geodetic data since the mid-1970s [6,46] or in situ glaciological measurements [2,11,50,84]. However, in situ measurements are scarce, and continued measurements from Himalayan glaciers are only available after 2000 and most geodetic studies investigate only two periods since the 1970s (e.g., [6,46]) or a few periods since 2000 [41]. We provide, in the studies performed within the Dragon 4 project and joint projects with Chinese colleagues, the most detailed time series since the 1960s for several regions across HMA. Hereby, we could show that increasing mass loss during the last 50 years is a general phenomenon and that mass loss now prevails, even in regions with formerly balanced mass budgets [47]. The only region with comparable information apart from this study is the Mt Everest region, where [36,48] show a similar steady increase of mass loss since the 1960s.

The loss of ice from glaciers in the Poiqu basin appears to have been driven by a combination of climatic and glaciological factors. Meteorological and reanalyses data suggest an increase (~0.2 °C) in summer (ablation season) temperatures as well as a decrease (~60 mm, 13%) in solid precipitation (accumulation) when comparing the periods covered by geodetic observations (1974–2004, 2004–2018). In situ measurements at Nielamu station showed precipitation variability along with significantly increased temperatures (Figure 7).

The analysis of the climate data also hint at extended ablation seasons. For the Mt Everest region, which has similar climatic and glaciological characteristics (Pelto et al., 2021), [85] found ablation seasons extending into mid-winter, as indicated by rising snow lines in recent years from October to January. These warmer post-monsoon and earl- winter periods can lead to significant sublimation, and hence increased mass loss (Potocki et al., 2022) [86].

The changes in temperature and precipitation correlate moderately (r^2 0.61–0.69) with glacier mass balance but do not explain the full variance of glacier mass budgets.

Proglacial lake development has also had a significant impact on glacier mass loss rates in the Poiqu basin, with the impact growing over time as lakes have expanded in the basin and lake-terminating glaciers having significantly more negative mass balances than the land-terminating one. Similar contrasts in the mass balance of glaciers of different terminus type were evident for all investigated study regions across the Himalaya [6]. T-values derived from the t-tests show the importance of terminus type on glacier mass budgets over the whole Himalaya for both time periods, with terminus type having a stronger influence on glacier mass balance between 2000 and 2015 (t- 10.04) compared to the period 1974–2000 (t- 4.07). Interestingly, there was little difference between mass loss rates from glaciers with and without substantial debris-cover in the Himalaya (mean difference -0.06, 95%, confidence range -0.10 to -0.02, t- 2.91–3.14) [6]. This is in line with previous independent studies [13,14], The analysis of the glacier velocity showed similar substantial differences between the lake- and land-terminating glaciers in the Poiqu basin. The analysis of more than 300 glaciers in different subregions along the Himalayan arc showed overall a slightly higher median velocity of 9.39 (interquartile range: 9.32–9.48) m yr^{-1} than in the Poiqu basin but a similar strong contrast between lake- and land-terminating glaciers. This indicates that dynamic thinning may play an important role for the mass loss of the lake-terminating glaciers [52]. The contrast also exists for debris-covered and debris-free glaciers. One of the main drivers of the dynamical thinning can be a reduction in basal friction due to the presence of the proglacial lake, which has also been postulated elsewhere [7,87,88].

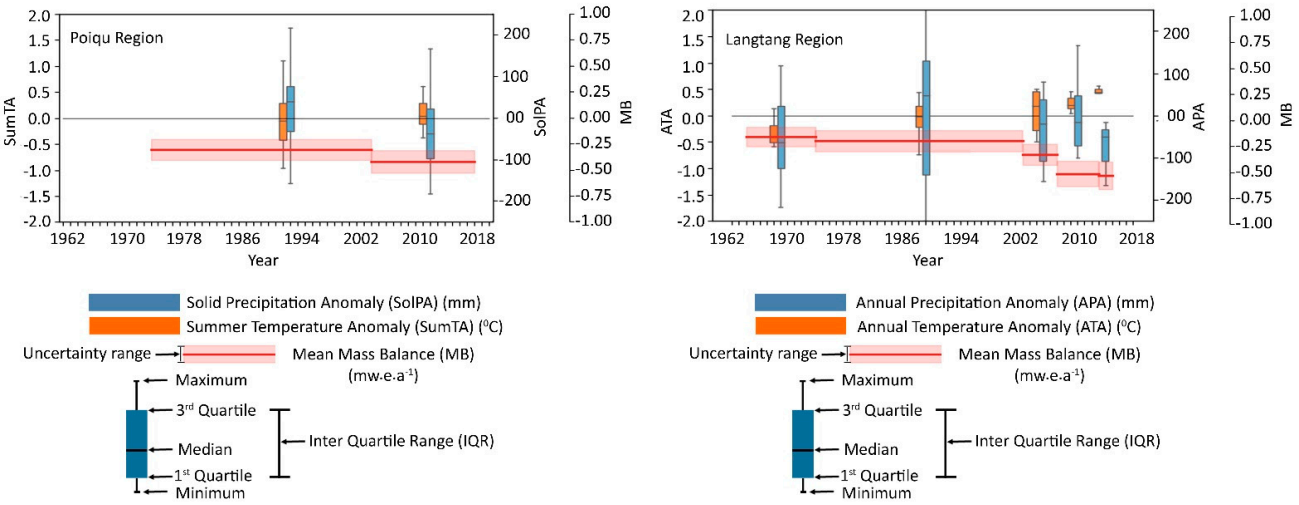

Figure 7. Comparison of average annual mass change rate of glaciers for the whole Poiqu Region with ERA5 Land climate variables and the mass change of the Langtang Basin with measurements at Nielamu station (adjusted based on [47]).

Our results emphasize the need for detailed assessment of past glacier behaviour in order to better calibrate and validate existing glacier models. While much emphasis has been put on understanding the influence of debris cover on glacier evolution (e.g., [10,89–91]), the results of our studies clearly show the importance of taking into account the presence and evolution of glacial lakes. This is true, even when considering that some lakes reached or will reach their potential maximum extent soon as more glacial lakes emerge with ongoing glacier wastage, as shown for the Poiqu basin and elsewhere in the Himalaya [49,92]. Simple parameterizations of processes such as glacier-lake interactions may need to be reassessed to improve the accuracy of glacier mass loss predictions, alongside glacier melt driven by further temperature increases. Current and future projections of melt water yield should also consider the potential ice stored in rock glaciers in permafrost environments, which are abundant but more resilient to climate chance [17,93].

Author Contributions: Conceptualization, T.B., G.Z., O.K., A.B., P.R. and J.B.P.; methodology, T.B., G.Z., O.K., A.B., P.R. and J.B.P.; data processing: A.B., O.K., J.B.P., P.R., G.Z. and Y.H.; formal analysis, O.K. and A.B.; writing—original draft preparation, T.B., O.K., J.B.P. and A.B.; writing—review and editing, all authors; visualization, O.K., T.B., A.B. and P.R.; supervision, T.B. and L.L.; project administration, T.B. and T.Y.; funding acquisition, T.B., T.Y. and L.L. All authors have read and agreed to the published version of the manuscript.

Funding: This research has been supported by the Dragon 4 program funded by ESA (4000121469/17/I-NB), the Swiss National Science Foundation (grant nos. IZLCZ2_169979/1 and 200021E_177652/1) and the Strategic Priority Research Program of Chinese Academy of Sciences (grant No. XDA20100300).

Institutional Review Board Statement: Not applicable.

Informed Consent Statement: Not applicable.

Data Availability Statement: The data produced within this study are either already available in open repositories (Pangaea: https://doi.pangaea.de/10.1594/PANGAEA.933924 or Zenodo: https://doi.org/10.5281/zenodo.4537289) and at www.mountcryo.org/datasets (last accessed 12 April 2022), or are available from the authors upon request.

Acknowledgments: We thank the reviewers for their constructive comments which helped to further improve the quality of this study.

Conflicts of Interest: The authors declare no conflict of interest.

References

1. Immerzeel, W.W.; Lutz, A.F.; Andrade, M.; Bahl, A.; Biemans, H.; Bolch, T.; Hyde, S.; Brumby, S.; Davies, B.J.; Elmore, A.C.; et al. Importance and vulnerability of the world's water towers. *Nature* **2020**, *577*, 364–369. [CrossRef] [PubMed]
2. Bolch, T.; Shea, J.M.; Liu, S.; Azam, F.M.; Gao, Y.; Gruber, S.; Immerzeel, W.W.; Kulkarni, A.; Li, H.; Tahir, A.A.; et al. Status and change of the cryosphere in the extended Hindu Kush Himalaya region. In *The Hindu Kush Himalaya Assessment: Mountains, Climate Change, Sustainability and People*; Wester, P., Mishra, A., Mukherji, A., Shrestha, A.B., Eds.; Springer International Publishing: Cham, Switzerland, 2019; pp. 209–255. ISBN 978-3-319-92288-1. [CrossRef]
3. Hock, R.; Rasul, G.; Adler, C.; Cáceres, B.; Gruber, S.; Hirabayashi, Y.; Jackson, M.; Kääb, A.; Kang, S.; Kutuzov, S.; et al. High Mountain Areas. In *IPCC Special Report on the Ocean and Cryosphere in a Changing Climate*; Pörtner, H.-O., Roberts, D.C., Masson-Delmotte, V., Thai, P., Tignor, M., Poloczanska, E., Mintenbeck, K., Alegría, A., Nicolai, M., Okem, A., et al., Eds.; University Press: Cambridge, UK; New York, NY, USA, 2019; pp. 131–202. [CrossRef]
4. Rounce, D.R.; Hock, R.; Shean, D.E. Glacier mass change in High Mountain Asia through 2100 using the open-source python glacier evolution model (PyGEM). *Front. Earth Sci.* **2020**, *7*, 331. [CrossRef]
5. Bolch, T. Asian glaciers are a reliable water source. *Nature* **2017**, *545*, 161–162. [CrossRef] [PubMed]
6. King, O.; Bhattacharya, A.; Bhambri, R.; Bolch, T. Glacial lakes exacerbate Himalayan glacier mass loss. *Sci. Rep.* **2019**, *9*, 18145. [CrossRef]
7. Sutherland, J.L.; Carrivick, J.L.; Gandy, N.; Shulmeister, J.; Quincey, D.J.; Cornford, S.L. Proglacial lakes control glacier geometry and behavior during recession. *Geophys. Res. Lett.* **2020**, *47*, e2020GL088865. [CrossRef]
8. Allen, S.K.; Zhang, G.; Wang, W.; Yao, T.; Bolch, T. Potentially dangerous glacial lakes across the Tibetan Plateau revealed using a large-scale automated assessment approach. *Sci. Bull.* **2019**, *64*, 435–445. [CrossRef]
9. Carrivick, J.L.; Tweed, F. A global assessment of the societal impacts of glacier outburst floods. *Glob. Planet. Change* **2016**, *144*, 1–16. [CrossRef]
10. Benn, D.I.; Bolch, T.; Hands, K.; Gulley, J.; Luckman, A.; Nicholson, L.I.; Quincey, D.; Thompson, S.; Toumi, R.; Wiseman, S. Response of debris-covered glaciers in the Mount Everest region to recent warming, and implications for outburst flood hazards. *Earth Sci. Rev.* **2012**, *114*, 156–174. [CrossRef]
11. Bolch, T.; Kulkarni, A.; Kääb, A.; Huggel, C.; Paul, F.; Cogley, J.G.; Frey, H.; Kargel, J.S.; Fujita, K.; Scheel, M.; et al. The state and fate of Himalayan glaciers. *Science* **2012**, *336*, 310–314. [CrossRef]
12. Herreid, S.; Pellicciotti, F. The state of rock debris covering Earth's glaciers. *Nat. Geosci.* **2020**, *13*, 621–627. [CrossRef]
13. Gardelle, J.; Berthier, E.; Arnaud, Y.; Kääb, A. Region-wide glacier mass balances over the Pamir–Karakoram–Himalaya during 1999–2011. *Cryosphere* **2013**, *7*, 1263–1286. [CrossRef]
14. Brun, F.; Wagnon, P.; Berthier, E.; Jomelli, V.; Maharjan, S.B.; Shrestha, F.; Kraaijenbrink, P.D.A. Heterogeneous influence of glacier morphology on the mass balance variability in High Mountain Asia. *J. Geophys. Res.* **2019**, *124*, 1331–1345. [CrossRef]
15. Jones, D.B.; Harrison, S.; Anderson, K.; Betts, R.A. Mountain rock glaciers contain globally significant water stores. *Sci. Rep.* **2018**, *8*, 2834. [CrossRef] [PubMed]
16. Jones, D.B.; Harrison, S.; Anderson, K.; Selley, H.L.; Wood, J.L.; Betts, R.A. The distribution and hydrological significance of rock glaciers in the Nepalese Himalaya. *Glob. Planet. Chang.* **2018**, *160*, 123–142. [CrossRef]
17. Janke, J.R.; Bolch, T. Rock glaciers. In *Treatise on Geomorphology*, 2nd ed.; Haritashya, U.K., Ed.; Elsevier: Amsterdam, The Netherlands, 2022. [CrossRef]
18. Haeberli, W.; Hallet, B.; Arenson, L.U.; Elconin, R.; Humlum, O.; Kääb, A.; Kaufmann, V.; Ladanyi, B.; Matsuoka, N.; Springman, S.; et al. Permafrost creep and rock glacier dynamics. *Permafr. Periglac. Process.* **2006**, *17*, 189–214. [CrossRef]
19. Paul, F.; Bolch, T.; Briggs, K.H.; Kääb, A.; McMillan, M.; McNabb, R.; Nagler, T.; Nuth, C.; Rastner, P.; Strozzi, T.; et al. Error sources and guidelines for quality assessment of glacier area, elevation change, and velocity products derived from satellite data in the Glaciers_cci project. *Remote Sens. Environ.* **2017**, *203*, 256–275. [CrossRef]
20. Westermann, S.; Duguay, C.R.; Grosse, G.; Kääb, A. Remote sensing of permafrost and frozen ground. In *Remote Sensing of the Cryosphere*; Tedesco, M., Ed.; Wiley: Hoboken, NJ, USA, 2015; pp. 307–344.
21. Wangchuk, S.; Bolch, T. Mapping of glacial lakes using Sentinel-1 and Sentinel-2 data and a random forest classifier: Strengths and challenges. *Sci. Remote Sens.* **2020**, *2*, 100008. [CrossRef]
22. Bolch, T.; Buchroithner, M.F.; Peters, J.; Baessler, M.; Bajracharya, S.R. Identification of glacier motion and potentially dangerous glacier lakes at Mt. Everest area/Nepal using spaceborne imagery. *Nat. Hazards Earth Syst. Sci.* **2008**, *8*, 1329–1340. [CrossRef]
23. Huggel, C.; Kääb, A.; Haeberli, W.; Teysseire, P.; Paul, F. Remote sensing-based assessment of hazards from glacier lake outbursts: A case study in the Swiss Alps. *Can. Geotech. J.* **2002**, *39*, 316–330. [CrossRef]
24. Paul, F. Changes in glacier area in Tyrol, Austria, between 1969 and 1992 derived from Landsat 5 TM and Austrian Glacier Inventory data. *Int. J. Remote Sens.* **2002**, *23*, 787–799. [CrossRef]
25. Bolch, T. Climate change and glacier retreat in northern Tien Shan (Kazakhstan/Kyrgyzstan) using remote sensing data. *Glob. Planet. Chang.* **2007**, *56*, 1–12. [CrossRef]
26. Zhang, G.; Yao, T.; Xie, H.; Wang, W.; Yang, W. An inventory of glacial lakes in the Third Pole region and their changes in response to global warming. *Glob. Planet. Chang.* **2015**, *131*, 148–157. [CrossRef]
27. Wang, X.; Guo, X.; Yang, C.; Liu, Q.; Wei, J.; Zhang, Y.; Liu, S.; Jiang, Z.; Tang, Z. Glacial lake inventory of high-mountain Asia in 1990 and 2018 derived from Landsat images. *Earth Syst. Sci. Data* **2020**, *12*, 2169–2182. [CrossRef]

28. Bolch, T.; Menounos, B.; Wheate, R.D. Landsat-based inventory of glaciers in western Canada, 1985–2005. *Remote Sens. Environ.* **2010**, *114*, 127–137. [CrossRef]
29. Shugar, D.H.; Burr, A.; Haritashya, U.K.; Kargel, J.S.; Watson, C.S.; Kennedy, M.C.; Bevington, A.R.; Betts, R.A.; Harrison, S.; Strattman, K. Rapid worldwide growth of glacial lakes since 1990. *Nat. Clim. Chang.* **2020**, *10*, 939–945. [CrossRef]
30. Pfeffer, W.T.; Arendt, A.A.; Bliss, A.; Bolch, T.; Cogley, J.G.; Gardner, A.S.; Hagen, J.-O.; Hock, R.; Kaser, G.; Kienholz, C.; et al. The Randolph Glacier Inventory: A globally complete inventory of glaciers. *J. Glaciol.* **2014**, *60*, 537–552. [CrossRef]
31. Dehecq, A.; Gourmelen, N.; Trouve, E. Deriving large-scale glacier velocities from a complete satellite archive: Application to the Pamir–Karakoram–Himalaya. *Remote Sens. Environ.* **2015**, *162*, 55–66. [CrossRef]
32. Scherler, D.; Leprince, S.; Strecker, M.R. Glacier-surface velocities in alpine terrain from optical satellite imagery—Accuracy improvement and quality assessment. *Remote Sens. Environ.* **2008**, *112*, 3806–3819. [CrossRef]
33. Heid, T.; Kääb, A. Evaluation of existing image matching methods for deriving glacier surface displacements globally from optical satellite imagery. *Remote Sens. Environ.* **2012**, *118*, 339–355. [CrossRef]
34. Paul, F.; Winsvold, H.S.; Kääb, A.; Nagler, T.; Schwaizer, G. Glacier remote sensing using Sentinel-2. Part II: Mapping glacier extents and surface facies, and comparison to Landsat 8. *Remote Sens.* **2016**, *8*, 575. [CrossRef]
35. Kääb, A.; Winsvold, H.S.; Altena, B.; Nuth, C.; Nagler, T.; Wuite, J. Glacier Remote Sensing Using Sentinel-2. Part I: Radiometric and Geometric Performance, and Application to Ice Velocity. *Remote Sens.* **2016**, *8*, 598. [CrossRef]
36. Bolch, T.; Pieczonka, T.; Benn, D.I. Multi-decadal mass loss of glaciers in the Everest area (Nepal, Himalaya) derived from stereo imagery. *Cryosphere* **2011**, *5*, 349–358. [CrossRef]
37. Berthier, E.; Cabot, V.; Vincent, C.; Six, D. Decadal region-wide and glacier-wide mass balances derived from multi-temporal ASTER satellite digital elevation models. Validation over the Mont-Blanc area. *Front. Earth Sci.* **2016**, *4*, 63. [CrossRef]
38. Dussaillant, I.; Berthier, E.; Brun, F.; Masiokas, M.; Hugonnet, R.; Favier, V.; Rabatel, A.; Pitte, P.; Ruiz, L. Two decades of glacier mass loss along the Andes. *Nat. Geosci.* **2019**, *12*, 802–808. [CrossRef]
39. Shean, D.E.; Bhushan, S.; Montesano, P.; Rounce, D.R.; Arendt, A.; Osmanoglu, B. A systematic, regional assessment of High Mountain Asia glacier mass balance. *Front. Earth Sci.* **2020**, *7*, 363. [CrossRef]
40. Sommer, C.; Malz, P.; Seehaus, T.C.; Lippl, S.; Zemp, M.; Braun, M.H. Rapid glacier retreat and downwasting throughout the European Alps in the early 21st century. *Nat. Commun.* **2020**, *11*, 3209. [CrossRef]
41. Hugonnet, R.; McNabb, R.; Berthier, E.; Menounos, B.; Nuth, C.; Girod, L.; Farinotti, D.; Huss, M.; Dussaillant, I.; Brun, F.; et al. Accelerated global glacier mass loss in the early twenty-first century. *Nature* **2021**, *592*, 726–731. [CrossRef]
42. Farr, T.G.; Rosen, P.A.; Caro, E.; Crippen, R.; Duren, R.; Hensley, S.; Kobrick, M.; Paller, M.; Rodriguez, E.; Roth, L.; et al. The Shuttle Radar Topography Mission. *Rev. Geophys.* **2007**, *45*, RG2004. [CrossRef]
43. Bolch, T.; Buchroithner, M.F.; Pieczonka, T.; Kunert, A. Planimetric and volumetric glacier changes in Khumbu Himalaya since 1962 using Corona, Landsat TM and ASTER data. *J. Glaciol.* **2008**, *54*, 592–600. [CrossRef]
44. Bhattacharya, A.; Bolch, T.; Mukherjee, K.; Pieczonka, T.; Kropáček, J.; Buchroithner, M.F. Overall recession and mass budget of Gangotri Glacier, Garhwal Himalayas, from 1965 to 2015 using remote sensing data. *J. Glaciol.* **2016**, *62*, 1115–1133. [CrossRef]
45. Pieczonka, T.; Bolch, T.; Wei, J.; Liu, S. Heterogeneous mass loss of glaciers in the Aksu-Tarim Catchment (Central Tien Shan) revealed by 1976 KH-9 Hexagon and 2009 SPOT-5 stereo imagery. *Remote Sens. Environ.* **2013**, *130*, 233–244. [CrossRef]
46. Maurer, J.M.; Schaefer, J.M.; Rupper, S.; Corley, A. Acceleration of ice loss across the Himalayas over the past 40 years. *Sci. Adv.* **2019**, *5*, eaav7266. [CrossRef] [PubMed]
47. Bhattacharya, A.; Bolch, T.; Mukherjee, K.; King, O.; Menounos, B.; Kapitsa, V.; Neckel, N.; Yang, W.; Yao, T. High Mountain Asian glacier response to climate revealed by multi-temporal satellite observations since the 1960s. *Nat. Commun.* **2021**, *12*, 4133. [CrossRef] [PubMed]
48. King, O.; Bhattacharya, A.; Ghuffar, S.; Tait, A.; Guilford, S.; Elmore, A.C.; Bolch, T. Six Decades of Glacier Mass Changes around Mt. Everest Are Revealed by Historical and Contemporary Images. *One Earth* **2020**, *3*, 608–620. [CrossRef]
49. Zhang, G.; Bolch, T.; Allen, S.; Linsbauer, A.; Chen, W.; Wang, W. Glacial lake evolution and glacier–lake interactions in the Poiqu River basin, central Himalaya, 1964–2017. *J. Glaciol.* **2019**, *65*, 347–365. [CrossRef]
50. Yao, T.; Thompson, L.G.; Yang, W.; Yu, W.; Gao, Y.; Guol, X.; Yang, X.; Duan, K.; Zhao, H.; Xu, B.; et al. Different glacier status with atmospheric circulations in Tibetan Plateau and surroundings. *Nat. Clim. Chang.* **2012**, *2*, 663–667. [CrossRef]
51. Rastner, P.; Bolch, T.; Hu, Y.; Liu, L.; Bhattacharya, A.; Zhang, G.; Yao, T. Occurrence and characteristics of rock glaciers in the Poiqu River basin—Central Himalaya. *Geogr. Ann. A* **2021**. *in review*. Available online: http://hdl.handle.net/10023/23838 (accessed on 4 December 2021).
52. Pronk, J.B.; Bolch, T.; King, O.; Wouters, B.; Benn, D.I. Contrasting surface velocities between lake- and land-terminating glaciers in the Himalayan region. *Cryosphere* **2021**, *15*, 5577–5599. [CrossRef]
53. Richardson, S.D.; Reynolds, J.M. An overview of glacial hazards in the Himalayas. *Quat. Int.* **2000**, *65–66*, 31–47. [CrossRef]
54. Wang, W.; Gao, Y.; Anacona, P.I.; Lei, Y.; Xiang, Y.; Zhang, G.; Li, S.; Lu, A. Integrated hazard assessment of Cirenmaco glacial lake in Zhangzangbo valley, Central Himalayas. *Geomorphology* **2018**, *306*, 292–305. [CrossRef]
55. Chen, X.; Cui, P.; Yang, Z.; Qi, Y. Risk assessment of glacial lake outburst in the Poiqu River basin of Tibet Autonomous region. *J. Glaciol. Geocryol.* **2007**, *29*, 509–516.
56. Zheng, G.; Allen, S.K.; Bao, A.; Ballesteros-Cánovas, J.A.; Huss, M.; Zhang, G.; Li, J.; Yuan, Y.; Jiang, L.; Yu, T.; et al. Increasing risk of glacial lake outburst floods from future Third Pole deglaciation. *Nat. Clim. Chang.* **2021**, *11*, 411–417. [CrossRef]

57. McFeeters, S.K. The use of the Normalized Difference Water Index (NDWI) in the delineation of open water features. *Int. J. Remote Sens.* **1996**, *17*, 1425–1432. [CrossRef]
58. Gardelle, J.; Arnaud, Y.; Berthier, E. Contrasted evolution of glacial lakes along the Hindu Kush Himalaya Mountain range between 1990 and 2009. *Glob. Planet. Change* **2011**, *75*, 47–55. [CrossRef]
59. Bolch, T.; Duethmann, D.; Wortmann, M.; Liu, S.; Disse, M. Declining glaciers endanger sustainable development of the oases along the Aksu-Tarim River (Central Asia). *Int. J. Sustain. Dev. World Ecol.* **2021**, *29*, 1–10. [CrossRef]
60. Pritchard, H.D. Asia's shrinking glaciers protect large populations from drought stress. *Nature* **2019**, *569*, 649–654. [CrossRef]
61. Thayyen, R.J.; Gergan, J.T. Role of glaciers in watershed hydrology: A preliminary study of a Himalayan catchment. *Cryosphere* **2010**, *4*, 115–128. [CrossRef]
62. Huss, M.; Hock, R. Global-scale hydrological response to future glacier mass loss. *Nat. Clim. Chang.* **2018**, *8*, 135–140. [CrossRef]
63. Nuth, C.; Kääb, A. Co-registration and bias corrections of satellite elevation data sets for quantifying glacier thickness change. *Cryosphere* **2011**, *5*, 271–290. [CrossRef]
64. McNabb, R.; Nuth, C.; Kääb, A.; Girod, L. Sensitivity of glacier volume change estimation to DEM void interpolation. *Cryosphere* **2019**, *13*, 895–910. [CrossRef]
65. Huss, M. Density assumptions for converting geodetic glacier volume change to mass change. *Cryosphere* **2013**, *7*, 877–887. [CrossRef]
66. Pieczonka, T.; Bolch, T. Region-wide glacier mass budgets and area changes for the Central Tien Shan between ~1975 and 1999 using Hexagon KH-9 imagery. *Glob. Planet. Chang.* **2015**, *128*, 1–13. [CrossRef]
67. Ragettli, S.; Bolch, T.; Pellicciotti, F. Heterogeneous glacier thinning patterns over the last 40 years in Langtang Himal, Nepal. *Cryosphere* **2016**, *10*, 2075–2097. [CrossRef]
68. Leprince, S.; Barbot, S.; Ayoub, F. Automatic and precise orthorectification, coregistration, and subpixel correlation of satellite images, application to ground deformation measurements. *IEEE Trans. Geosci. Remote Sens.* **2007**, *45*, 1529–1558. [CrossRef]
69. Heid, T.; Kääb, A. Repeat optical satellite images reveal widespread and long term decrease in land-terminating glacier speeds. *Cryosphere* **2012**, *6*, 467–478. [CrossRef]
70. Dehecq, A.; Gourmelen, N.; Gardner, A.S.; Brun, F.; Goldberg, D.; Nienow, P.W.; Berthier, E.; Vincent, C.; Wagnon, P.; Trouvé, E. Twenty-first century glacier slowdown driven by mass loss in High Mountain Asia. *Nat. Geosci.* **2019**, *12*, 22–27. [CrossRef]
71. Willis, M.J.; Melkonian, A.K.; Pritchard, M.E.; Ramage, J.M. Ice loss rates at the Northern Patagonian Icefield derived using a decade of satellite remote sensing. *Landsat Sci. Results* **2012**, *117*, 184–198. [CrossRef]
72. Guizar-Sicairos, M.; Thurman, S.T.; Fienup, J.R. Efficient subpixel image registration algorithms. *Opt. Lett.* **2008**, *33*, 156–158. [CrossRef]
73. Barsch, D. *Rockglaciers: Indicators for the Present and Former Geoecology in High Mountain Environments*; Springer: Berlin/Heidelberg, Germany, 1996; ISBN 3-540-60742-0.
74. Berthling, I. Beyond confusion: Rock glaciers as cryo-conditioned landforms. *Geomorphology* **2011**, *131*, 98–106. [CrossRef]
75. Brighenti, S.; Tolotti, M.; Bruno, M.C.; Engel, M.; Wharton, G.; Cerasino, L.; Mair, V.; Bertoldi, W. After the peak water: The increasing influence of rock glaciers on alpine river systems. *Hydrol. Process.* **2019**, *33*, 2804–2823. [CrossRef]
76. Reinosch, E.; Gerke, M.; Riedel, B.; Schwalb, A.; Ye, Q.; Buckel, J. Rock glacier inventory of the western Nyainqêntanglha Range, Tibetan Plateau, supported by InSAR time series and automated classification. *Permafr. Periglac. Process.* **2021**, *32*, 657–672. [CrossRef]
77. Blöthe, J.H.; Rosenwinkel, S.; Höser, T.; Korup, O. Rock-glacier dams in High Asia. *Earth Surf. Process. Landf.* **2019**, *44*, 808–824. [CrossRef]
78. Bolch, T.; Rohrbach, N.; Kutuzov, S.; Robson, B.A.; Osmonov, A. Occurrence, evolution and ice content of ice-debris complexes in the Ak-Shiirak, Central Tien Shan revealed by geophysical and remotely-sensed investigations. *Earth Surf. Process. Landf.* **2019**, *44*, 129–143. [CrossRef]
79. Brardinoni, F.; Scotti, R.; Sailer, R.; Mair, V. Evaluating sources of uncertainty and variability in rock glacier inventories. *Earth Surf. Process. Landf.* **2019**, *44*, 2450–2466. [CrossRef]
80. Robson, B.A.; Bolch, T.; MacDonell, S.; Hölbling, D.; Rastner, P.; Schaffer, N. Automated detection of rock glaciers using deep learning and object-based image analysis. *Remote Sens. Environ.* **2020**, *250*, 112033. [CrossRef]
81. Nie, Y.; Sheng, Y.; Liu, Q.; Liu, L.; Liu, S.; Zhang, Y.; Song, C. A regional-scale assessment of Himalayan glacial lake changes using satellite observations from 1990 to 2015. *Remote Sens. Environ.* **2017**, *189*, 1–13. [CrossRef]
82. Brun, F.; Berthier, E.; Wagnon, P.; Kääb, A.; Treichler, D. A spatially resolved estimate of High MountainAsia glacier mass balances from 2000 to 2016. *Nat. Geosci.* **2017**, *10*, 668–673. [CrossRef]
83. Zemp, M.; Huss, M.; Thibert, E.; Eckert, N.; McNabb, R.; Huber, J.; Barandun, M.; Machguth, H.; Nussbaumer, S.U.; Gärtner-Roer, I.; et al. Global glacier mass changes and their contributions to sea-level rise from 1961 to 2016. *Nature* **2019**, *568*, 382–386. [CrossRef]
84. Azam, M.F.; Wagnon, P.; Berthier, E.; Vincent, C.; Fujita, K.; Kargel, J.S. Review of the status and mass changes of Himalayan-Karakoram glaciers. *J. Glaciol.* **2018**, *64*, 61–74. [CrossRef]
85. Pelto, M.; Panday, P.; Matthews, T.; Maurer, J.; Perry, L.B. Observations of winter ablation on glaciers in the mount everest region in 2020–2021. *Remote Sens.* **2021**, *13*, 2692. [CrossRef]

86. Potocki, M.; Mayewski, P.A.; Matthews, T.; Perry, L.B.; Schwikowski, M.; Tait, A.M.; Korotkikh, E.; Clifford, H.; Kang, S.; Sherpa, T.C.; et al. Mt. Everest's highest glacier is a sentinel for accelerating ice loss. *npj Clim. Atmos. Sci.* **2022**, *5*, 7. [CrossRef]
87. Tsutaki, S.; Fujita, K.; Nuimura, T.; Sakai, A.; Sugiyama, S.; Komori, J.; Tshering, P. Contrasting thinning patterns between lake- and land-terminating glaciers in the Bhutanese Himalaya. *Cryosphere* **2019**, *13*, 2733–2750. [CrossRef]
88. Carrivick, J.L.; Tweed, F.S.; Sutherland, J.L.; Mallalieu, J. Toward numerical modeling of interactions between ice-marginal proglacial lakes and glaciers. *Front. Earth Sci.* **2020**, *8*, 577068. [CrossRef]
89. Anderson, L.S.; Anderson, R.S. Modeling debris-covered glaciers: Response to steady debris deposition. *Cryosphere* **2016**, *10*, 1105–1124. [CrossRef]
90. Mölg, N.; Fergusson, J.; Bolch, T.; Vieli, A. On the influence of debris cover on glacier morphology: How high-relief structures evolve from smooth surfaces. *Geomorphology* **2020**, *357*, 107092. [CrossRef]
91. Miles, E.S.; Pellicciotti, F.; Willis, I.C.; Steiner, J.F.; Buri, P.; Arnold, N.S. Refined energy-balance modelling of a supraglacial pond, Langtang Khola, Nepal. *Ann. Glaciol.* **2016**, *57*, 29–40. [CrossRef]
92. Linsbauer, A.; Frey, H.; Haeberli, W.; Machguth, H.; Azam, M.F.; Allen, S. Modelling glacier-bed overdeepenings and possible future lakes for the glaciers in the Himalaya–Karakoram region. *Ann. Glaciol.* **2016**, *57*, 117–130. [CrossRef]
93. Harrison, S.; Jones, D.; Anderson, K.; Shannon, S.; Betts, R.A. Is ice in the Himalayas more resilient to climate change than we thought? *Geogr. Ann. A* **2021**, *103*, 1–7. [CrossRef]